JACS
JOURNAL OF THE AMERICAN CHEMICAL SOCIETY

ARTICLE

pubs.acs.org/JACS

Rotation Mechanism of F_1-ATPase: Crucial Importance of the Water Entropy Effect

Takashi Yoshidome,[†] Yuko Ito,[‡] Mitsunori Ikeguchi,[‡] and Masahiro Kinoshita*[,†]

[†]Institute of Advanced Energy, Kyoto University, Uji, Kyoto 611-0011, Japan

[‡]Graduate School of Nanobioscience, Yokohama City University, 1-7-29, Suehiro-cho, Tsurumi-ku, Yokohama 230-0045, Japan

Supporting Information

ABSTRACT: We propose a novel picture of the rotation mechanism of F_1-ATPase, a rotary-motor protein complex. Entropy, which originates from the translational displacement of water molecules, is treated as the key factor in the proposal. We calculate the water entropy gains upon formation of the $\alpha-\beta$, $\alpha-\gamma$, and $\beta-\gamma$ subunit pairs. The gain is given as the difference between the hydration entropy of a subunit pair and the sum of the hydration entropies of the separate subunits forming the pair. The calculation is made using a hybrid of a statistical-mechanical theory for molecular liquids and morphometric approach. The water entropy gain is considered as a measure of tightness of the packing at each subunit interface. The results are highly correlated with the numbers of stable contacts at the subunit interfaces estimated by a molecular dynamics simulation. We also calculate the hydration entropies of three different subcomplexes comprising the γ subunit, one of the β subunits, and two α subunits adjacent to them. The major finding is that the packing in F_1-ATPase is highly asymmetrical, and this asymmetry is ascribed to the water entropy effect. We discuss how the rotation of the γ subunit is induced by such chemical processes as ATP binding, ATP hydrolysis, and release of the products. In our picture, the asymmetrical packing plays crucially important roles, and the rotation is driven by the water entropy effect.

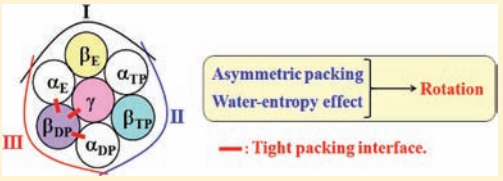

INTRODUCTION

Adenosine triphosphate (ATP) is a universal currency of energy in living organisms. Motor proteins, which play imperative roles in sustaining life, function through their large conformational changes induced by such chemical processes as ATP binding, ATP hydrolysis, and release of products [adenosine diphosphate (ADP) and inorganic phosphate (Pi)]. It is of central interest to elucidate how the conformational changes are coupled with the chemical processes. The elucidation would provide important progress toward understanding the functional mechanisms of motor proteins. F_1-ATPase, a soluble part in F_oF_1-ATP synthase, is a rotary motor that has been studied extensively in experiments: a number of three-dimensional structures have been solved using X-ray crystallography;[1−6] the rotation of the central stalk (i.e., γ subunit) of F_1-ATPase has directly been observed in single-molecule experiments;[7−21] and the correspondence between the chemical processes and the rotational angles of the central stalk has been made rather clear.[10−16] Furthermore, F_1-ATPase is capable of catalyzing the reverse reaction (i.e., ATP synthesis) when the central stalk is forced to rotate in the direction opposite to the case of ATP hydrolysis.[22] This is indicative of the tight coupling of the chemical processes and the conformational changes of F_1-ATPase. Thus, F_1-ATPase is well suited for investigation of the coupling scheme in atomic detail using state-of-the-art theoretical methods.

F_1-ATPase is a complex of proteins comprising several subunits. The minimum complex of F_1-ATPase needed for the rotation is the $\alpha_3\beta_3\gamma$ complex[7] considered in the present article. According to the atomic-level crystal structures of the $\alpha_3\beta_3\gamma$ complex,[1−5] the $\alpha_3\beta_3$ subunits are arranged hexagonally around the γ subunit, as shown in Figure 1. During the cycle of the chemical processes explained in the first paragraph, the γ subunit rotates in a counterclockwise direction when it is viewed from the F_o side.[7] The following experimental results have been reported: (i) the γ subunit performs a 120° step rotation during hydrolysis of a single ATP molecule,[8] and (ii) the step is further resolved into 80° and 40° substeps.[9] The 80° substep is induced by ATP binding.[9] Subsequent ATP hydrolysis occurs in 1 ms without rotation,[10] followed by a 40° rotation accompanying release of Pi.[12] The 80° and 40° substeps are referred to as catalytic and ATP-waiting dwells, respectively.

The crystal structure reported by Abrahams et al.[1] is illustrated in Figure 1. Adenosine-5′-(β,γ-imino)-triphosphate (AMP-PNP), an analogue of ATP, and ADP are bound to the β subunits named β_{TP} and β_{DP}, respectively. Nothing is bound to the β subunit named β_E. (The three α subunits are named α_{TP}, α_{DP}, and α_E, respectively, as shown in the figure.[1]) The catalytic site within each β subunit is located at the interface between α and β subunits (a residue of α_{DP} strongly interacts with the nucleotide bound to β_{DP}). Though the conformations of the three α subunits are almost the same, those of the β subunits are significantly different from one another: β_{TP} and β_{DP} are in closed conformations, while β_E takes an open conformation. Most of the crystal structures that have been reported so far represent essentially the same characteristics, though the

Received: November 3, 2010
Published: February 24, 2011

ACS Publications © 2011 American Chemical Society

dx.doi.org/10.1021/ja109594y | J. Am. Chem. Soc. 2011, 133, 4030–4039

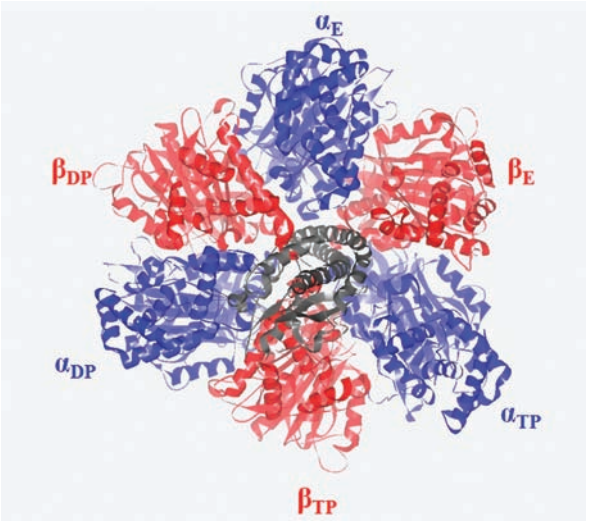

Figure 1. Ribbon representation of the $\alpha_3\beta_3\gamma$ complex viewed from the F_o side.[1] The α and β subunits are alternately arranged around the γ subunit represented by the black ribbon. The γ subunit rotates in a counterclockwise direction.[7] This figure is drawn using the DS visualizer 2.5.

substrates bound are different.[2,5] The 120° rotation of the γ subunit is induced by the interconversion of the β-subunit structures ($\beta_{DP}\rightarrow\beta_E$, $\beta_{TP}\rightarrow\beta_{DP}$, and $\beta_E\rightarrow\beta_{TP}$). The structures of the $\alpha_3\beta_3\gamma$ complex before and after the 120° rotation are the same. According to single-molecule experiments,[14−16] most of the crystal structures are in the catalytic dwell state. This implies that the 40° rotation occurs first from the crystal structure, and the 80° rotation is then induced by the ATP binding.

Despite an enormous amount of investigation using single-molecule experiments,[7−22] X-ray crystallography,[1−6] and molecular dynamics (MD) simulations,[23−32] the microscopic mechanism of the rotation has not been elucidated yet. In our opinion, the direct interactions (or the screened electrostatic interactions) among the subunits have been treated as the dominant factors, while the roles of water have caught much less attention. Here we suggest a completely different concept: The rotation of the γ subunit is controlled primarily by the entropic effect originating from the translational displacement of water molecules.

Our recent theoretical analyses based on statistical thermodynamics have shown that the water entropy is the key quantity in elucidating the folding/unfolding mechanisms of proteins.[33−51] For example, the backbone and side chains of a protein generate excluded volumes (EVs) which the centers of water molecules cannot enter.[33,34] Upon protein folding, the EVs overlap, leading to a decrease in the total EV (see Figure 2). This decrease provides a corresponding increase in the total volume available to the translational displacement of the coexisting water molecules and in the number of accessible configurations of the water. Thus, protein folding accompanies a water entropy gain (in a strict sense, the gain is affected not only by the EV but also by the other geometric measures as described in the Morphometric Approach section). The reduction of the EV and the water entropy gain become substantially large when the backbone and side chains are tightly packed.

Experimental studies support our concept described above: It has been shown that, in protein folding,[52] receptor−ligand binding,[53] amyloid−fibril formation,[54] association of viruses,[55]

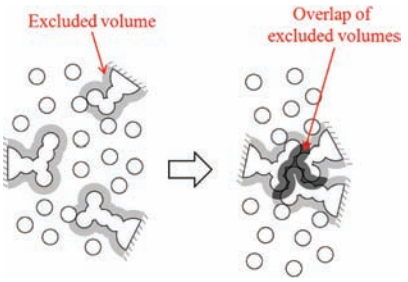

Figure 2. Close packing of three side chains. The excluded volume generated by a side chain is the volume occupied by the side chain itself plus the volume shown in gray. When side chains are closely packed, the excluded volumes overlap. The total volume available to the translational displacement of water molecules increases by the overlapped volume shown in black, leading to a water entropy gain.

and formation of actin filaments,[56,57] the enthalpic and entropic changes are both positive at ambient temperature and pressure, proving that these processes are entropically driven. We have recently succeeded in reproducing *quantitatively* the experimentally measured changes in the thermodynamic quantities upon the folding of apoplastocyanin (apoPC)[52] by our theoretical method which fully accounts for the water entropy effect.[37] According to the usual view,[58] the water adjacent to a nonpolar group is entropically unstable, and protein folding is driven by the release of such unfavorable water to the bulk through the burial of nonpolar groups. We have shown, however, that the entropic gain originating from this view is too small to elucidate the water entropy gain manifesting the apoPC-folding data.[37]

In the present article, we report a novel picture of the rotation mechanism of F_1-ATPase based on the water entropy effect. The hydration entropy (HE) of a large solute with a prescribed structure is calculated using the angle-dependent integral equation theory[59−61] combined with the multipolar water model,[62,63] a statistical-mechanical theory for molecular liquids, and the morphometric approach.[64,65] We calculate the water entropy changes upon the formation of the $\alpha-\beta$, $\alpha-\gamma$, and $\beta-\gamma$ subunit pairs. The change is given as the difference between the HE of a subunit pair and the sum of the hydration entropies of the separate subunits forming the pair. The results are in an excellent correlation with those obtained by a MD simulation,[32] demonstrating the validity of our theoretical approach focused on the water entropy effect (a summary of the results of the MD simulation[32] is given in the next section). It is remarkable that the framework of the results obtained by the MD simulation with an arduous computational effort can be reproduced using our theoretical approach, in which the water entropy change upon formation of a subunit pair is calculated in only a few seconds. We also calculate the hydration entropies of three different subcomplexes comprising the γ subunit, one of the β subunits, and two α subunits adjacent to them. On the basis of the results obtained, we point out that the packing in the $\alpha_3\beta_3\gamma$ complex is highly asymmetrical and that the asymmetric packing plays crucially important roles in the rotation of the γ subunit. We reach the novel picture of the rotation mechanism by arguing how the rotation of the γ subunit is induced by the chemical processes of ATP binding, ATP hydrolysis, and release of the products. In this picture, the asymmetrical packing plays crucially important roles, and the rotation is driven by the water entropy effect.

dx.doi.org/10.1021/ja109594y |*J. Am. Chem. Soc.* 2011, 133, 4030–4039

Table 1. Numbers of Stable Contacts of Subunit Pairs Estimated by Ito and Ikeguchi's MD Simulation with All-Atom Potentials[32a]

α−β subunit pairs		α−γ subunit pairs		β−γ subunit pairs	
$\alpha_E-\beta_E$	56	$\alpha_E-\gamma$	13	$\beta_E-\gamma$	19
$\alpha_{TP}-\beta_{TP}$	74	$\alpha_{TP}-\gamma$	6	$\beta_{TP}-\gamma$	7
$\alpha_{DP}-\beta_{DP}$	78	$\alpha_{DP}-\gamma$	6	$\beta_{DP}-\gamma$	14
$\alpha_E-\beta_{DP}$	68				
$\alpha_{TP}-\beta_E$	41				
$\alpha_{DP}-\beta_{TP}$	54				

[a] In the estimation,[66] the authors detect the inter-subunit residue pairs maintaining their inter-atomic distances less than 4.5 Å for 98% of the snapshots in the MD trajectory.

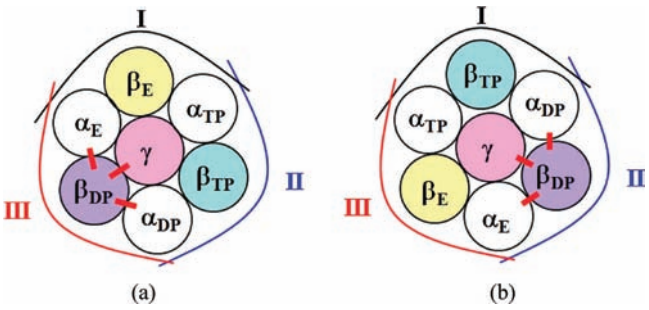

Figure 3. Schematic representations of (a) the crystal structure shown in Figure 1 and (b) the structure after the 120° rotation of the γ subunit. The red lines represent that the packing in two adjacent subunits is especially tight.[32] Three circular arcs denote subcomplexes I (black), II (blue), and III (red), respectively. The subcomplexes are defined in the Model and Theoretical Approach section.

■ ASYMMETRIC NATURE OF INTERFACES BETWEEN ADJACENT SUBUNITS IN F_1-ATPASE

Ito and Ikeguchi[32] have performed an MD simulation with all-atom potentials comprising Lennard-Jones and Coulomb terms for the $\alpha_3\beta_3\gamma$ complex with the crystal structure of bovine heart mitochondria (PDB ID: 2JDI).[5] Their results are summarized in Table 1 and Figure 3a. The stable contacts in Table 1 are defined as the inter-subunit residue pairs maintaining their inter-atomic distances less than 4.5 Å for 98% of the snapshots in the MD trajectory.[66] The number of stable contacts represents a measure of the tightness of interface packing between adjacent subunits. It follows from Table 1 that the measure varies considerably from interface to interface. The packing in β_{DP}, adjacent α subunits, and the γ subunit is especially tight, as observed in Figure 3, implying that the four subunits are strongly interacting. Experimental studies have shown that, in the structure illustrated in Figure 1, rotation of the γ subunit occurs upon a structural change of β_{DP}, the catalytically active subunit.[16] It is likely that perturbation of the tight packing by the structural change of β_{DP} induces the movement of the γ subunit.

■ MODEL AND THEORETICAL APPROACH

Protein Model. For the $\alpha_3\beta_3\gamma$ complex, we use the crystal structure employed by Ito and Ikeguchi.[32] The missing residues (α_{TP}402−409, β_E388−395, γ48−66, 87−104, 117−126, 149−158, and 174−205) are added using MODELLER[67] on the basis of the crystal structure, whose PDB ID is 1E79.[2] The total number of atoms is ∼49 000. In the crystal structure, all subunits except for β_E have AMP-PMP and Mg^{2+}. Neither the nucleotide nor Mg^{2+} is bound to β_E. We replace AMP-PMP with ATP because the results of single-molecule experiments have indicated that most of the crystal structures are in the catalytic dwell state.[14−16] The resultant structure is optimized using a standard energy-minimization technique.[32]

In the present study, we calculate the HE S, which represents the water entropy loss upon the insertion of a solute with a prescribed structure. A larger absolute value of S means a larger magnitude of the loss. In general, the hydration energy is largely dependent on the solute−water interaction potentials, while S is not.[41,68] For example, Imai et al.[68] considered the native structures of a total of eight peptides and proteins and calculated S using the three-dimensional reference interaction site model (3D-RISM) theory combined with all-atom potentials comprising Lennard-Jones and Coulomb terms and the SPC/E water model. Even when the protein−water electrostatic potentials, which are quite strong, are shut off and only the LJ potentials are retained, S decreases by <5%. Thus, we can adopt a simplified model for the protein−water interaction potentials in calculating S: we model a protein and ATP as a set of fused hard spheres, and Mg^{2+} as a hard sphere. This type of modeling can also be justified as follows. The hydration free energy μ, entropy S, and energy U are calculated for a spherical solute with diameter 0.28 nm using the angle-dependent integral equation theory[59−61] combined with the multipolar water model.[62,63] For the hard-sphere solute with zero charge, the calculated values are $\mu = 5.95k_BT$, $S = -9.22k_B$, and $U = -3.27k_BT$. When the point charge $-0.5e$ (e is the electronic charge) is embedded at its center, the calculated values are $\mu = -32.32k_BT$, $S = -10.11k_B$, and $U = -42.43k_BT$. Thus, S is fairly insensitive to the solute−water interaction potential, while μ and U are largely influenced by it. Since what we calculate in this article is S, the solutes can be modeled as a set of fused hard spheres or as a hard sphere. The polyatomic structure, which is crucially important, is accounted for on the atomic level: all of the atoms constructing the protein complex and ATP (i.e., hydrogen, oxygen, carbon, nitrogen, sulfur, and phosphorus) are incorporated in the structures. The diameter of each atom is set at the σ-value of the Lennard-Jones potential parameters which are taken from CHARMM22.[69] In the calculation of HE, the (x,y,z)-coordinates of solute atoms are used as part of the input data to characterize each structure. The water entropy change upon the conformational change of a solute from structure A to structure B is equal to the HE of structure B minus that of structure A.

In accordance with the MD simulation by Ito and Ikeguchi,[32] we define the following three subcomplexes for the arrangement shown in Figure 3a:

- Subcomplex I: γ, β_E, α_E, and α_{TP}
- Subcomplex II: γ, β_{TP}, α_{TP}, and α_{DP}
- Subcomplex III: γ, β_{DP}, α_{DP}, and α_E

We name the subcomplexes in terms of their positions in the crystal structure. For example, when the γ subunit rotates by 120° (see Figure 3b), the arrangement changes and subcomplex III now comprises γ, β_E, α_E, and α_{TP}. We calculate the HEs not only of the three subcomplexes but also of α, β, and γ subunits and of α−β, α−γ, and β−γ subunit pairs. We define $\Delta S_{ij}/k_B$ as

$$\Delta S_{ij}/k_B \equiv S_{ij}/k_B - S_i/k_B - S_j/k_B \quad (1)$$

Here, S_{ij} is the HE of subunit pair i−j and S_i is the HE of subunit i (i = α_E, α_{TP}, α_{DP}, β_E, β_{TP}, and β_{DP}; Subunit j is the subunit adjacent to subunit i). ΔS_{ij} represents the water entropy gain upon formation of subunit pair i−j. It becomes larger as the tightness of interface packing between subunit pair i−j increases. Thus, $\Delta S_{ij}/k_B$ is a measure of the tightness like the number of stable contacts

dx.doi.org/10.1021/ja109594y |J. Am. Chem. Soc. 2011, 133, 4030–4039

calculated in the MD simulation.[32] There is no ATP-Mg^{2+} bound to β_E. Hence, β_E has fewer atoms than the other β subunits. To extract the effect of the interface packing impartially, we calculate the HE of ATP-Mg^{2+} and add it to the HEs of β_E, $\alpha_{DP}-\beta_E$, $\alpha_E-\beta_E$, and $\gamma-\beta_E$ subunit pairs and subcomplex I.

Angle-Dependent Integral Equation Theory. We employ a multipolar model for water.[62,63] A water molecule is modeled as a hard sphere with diameter 0.28 nm in which a point dipole and a point quadrupole of tetrahedral symmetry are embedded. The effect of the molecular polarizability is taken into account using the self-consistent mean field (SCMF) theory.[62,63] At the SCMF level, the many-body induced interactions are reduced to pairwise additive potentials involving an effective dipole moment. Since the molecular model is employed for water, the angle-dependent version[59−61] must be used for the integral equation theory for incorporating the orientational correlations (details of the angle-dependent integral equation theory and the multipolar water model are given in the Supporting Information). The validity of the angle-dependent integral equation theory has been verified in a number of applications. For example, the hydration free energies of small nonpolar solutes calculated by the theory combined with the multipolar water model are in perfect agreement with those from Monte Carlo simulations with the SPC/E and TIP4P water models.[60] The dielectric constant for bulk water, which is determined from the water−water orientational correlation functions, is in good agreement with the experimental data.[60] The theory is also capable of elucidating the hydrophilic hydration experimentally known.[61] Despite these successful results, the application of the theory to complex solute molecules like proteins is rather difficult due to the mathematical complexity. This problem can be overcome by combining it with the morphometric approach.[64,65]

Morphometric Approach. In the morphometric approach,[64,65] any of the hydration thermodynamic quantities is expressed using only four geometric measures of a solute with a fixed structure and corresponding coefficients. The resultant morphometric form for the HE is given by

$$S/k_B = C_1V_{ex} + C_2A + C_3X + C_4Y \quad (2)$$

Here, V_{ex} is the EV, A is the water-accessible surface area (ASA), and X and Y are the integrated mean and Gaussian curvatures of the water-accessible surface, respectively; these are the four geometric measures used. The Boltzmann constant is denoted by k_B. The water-accessible surface is the surface that is accessible to the centers of water molecules.[70] ASA, X, and Y are the surface area and the integrated curvatures of the water-accessible surface, respectively. The EV is the volume that is enclosed by the accessible surface.[65] We calculate the four geometric measures by extension[65] of Connolly's algorithm.[71,72] In this approach, the solute shape enters S/k_B only via the four geometric measures. Therefore, the four coefficients (C_1-C_4) can be determined in simple geometries. They are calculated from the values of S/k_B for hard-sphere solutes with various diameters immersed in our model water. The angle-dependent integral equation theory[59−61] combined with the multipolar water model[62,63] is employed in the calculation. More details are available in our earlier publications[37,49] and in the Supporting Information.

The high usefulness of the morphometric approach has already been demonstrated. For example, the results from the 3D integral equation theory[73,74] applied to the same model protein immersed in a simple solvent (in which the solvent particles interact through strongly attractive potential as water molecules) can be reproduced with sufficient accuracy by the morphometric approach applied to the same solvent.[38] By a hybrid of the angle-dependent integral equation theory combined with the multipolar water model and the morphometric approach, the experimentally measured changes in thermodynamic quantities upon apoPC folding are quantitatively reproduced.[37]

Table 2. Water Entropy Gain upon the Formation of Subunit Pair $i-j$, $\Delta S_{ij}/k_B$[a]

$\alpha-\beta$ subunit pair		$\alpha-\gamma$ subunit pair		$\beta-\gamma$ subunit pair	
$\alpha_E-\beta_E$	230.0	$\alpha_E-\gamma$	68.5	$\beta_E-\gamma$	65.4
$\alpha_{TP}-\beta_{TP}$	381.9	$\alpha_{TP}-\gamma$	17.5	$\beta_{TP}-\gamma$	37.8
$\alpha_{DP}-\beta_{DP}$	514.0	$\alpha_{DP}-\gamma$	4.50	$\beta_{DP}-\gamma$	88.5
$\alpha_E-\beta_{DP}$	283.8				
$\alpha_{TP}-\beta_E$	199.9				
$\alpha_{DP}-\beta_{TP}$	291.9				

[a] The gain is given as the difference between the hydration entropy of a subunit pair and the sum of the hydration entropies of separate subunits forming the pair (see eq 2).

Moreover, great progress has been made in elucidating the microscopic mechanisms of pressure,[42−47] cold,[48,49] and heat[50,51] denaturating of proteins and in the prediction of the native structure[35,36,40] by our theoretical methods in which the morphometric approach is combined with the integral equation theory or its angle-dependent version.

Importance of Protein−Water−Water Triplet and Higher-Order Correlations for the Hydration Entropy. As mentioned above, in the conventional view the HE of a protein stems from the changed hydrogen-bonding of the water network near the protein surface.[58] The HE is discussed primarily in terms of the protein−water orientational correlations and restriction of the rotational freedom of water molecules. For example, the experimental result for the GTP hydrolysis in the Ras-RasGAP complex was interpreted from such a viewpoint.[75] In our view, on the other hand, there is a factor which predominates over the conventionally argued one: Upon the insertion of a protein, the total volume available to the translational displacement of water molecules is reduced (i.e., the translational freedom of water molecules is restricted), leading to a decrease in the number of accessible configurations of water and a corresponding entropic loss. The effect of the insertion reaches water within a far larger length scale.[38,39] The first term in the morphometric form for the HE, which can be scaled by the EV, is the most important at ambient temperature and pressure. According to the Asakura−Oosawa (AO) theory,[76,77] which is widely used as a convenient way of estimating the first term, the HE is given by $-k_B\rho_S V_{ex}$, where ρ_S is the number density of bulk water. Lazaridis and Paulaitis[78,79] have proposed a theory in which the HE is calculated from a computer simulation and decomposed into the translational and orientational components. However, these theories account for only the protein−water pair correlation component.[44,45] We have shown for the translational entropy of water that the protein−water−water triplet and higher-order correlation components are substantially larger.[44] The presence of a water molecule generates an EV for the other water molecules in the system. This water crowding (i.e., water−water translational correlations) becomes more serious by the insertion, giving rise to a loss of the water entropy. This effect is ascribed to the protein−water multibody correlations.

The protein−water multibody correlations are incorporated in the formulations of the angle-dependent integral equation theory we employ. When the AO theory is applied to the calculation of the HE S of subcomplex III, for example, the result is $\sim -10\,600k_B$, which is unacceptably underestimated (this number is to be compared to that given in Table 3, $\sim -60\,600k_B$). We remark that the protein−water orientational correlations (at pair and multibody levels) as well as the translational correlations are taken into account in our theory. The orientational correlations are significantly large only in the close vicinity of the protein surface, which is in contrast to the translational correlations. Thus, the conventionally argued effect described at the beginning of this section, though it is less important, is also incorporated. Despite the fact that the translational and orientational correlations at pair and

Table 3. Hydration Entropy, S/k_B, Intra-subunit Contribution, Inter-subunit Contribution, and Number of Stable Contacts for Each Subcomplex[a]

	subcomplex I	subcomplex II	subcomplex III
S/k_B	−61 244.9 (−626)	−61 027.9 (−409)	−60 619.1 (0)
intra-subunit contribution	−61 826.8 (−235)	−61 760.7 (−169)	−61 592.2 (0)
inter-subunit contribution	581.9 (−391)	732.8 (−240)	973.1 (0)
no. of stable contacts	135	147	179

[a] The subcomplexes are defined in Model and Theoretical Approach. The intra-subunit contribution is the sum of the hydration entropies of subunits forming each subcomplex. The inter-subunit contribution is the difference between S/k_B and the intra-subunit contribution: this represents the contribution from the interface packing between subunits and can be a measure of tight packing like the number of stable contacts. The number of stable contacts in this table is defined as the sum of the numbers of stable contacts between subunits in each subcomplex. The value for a subcomplex relative to that for subcomplex III is given in parentheses.

multibody levels are all taken into consideration, the HE of a large protein or a complex of proteins can be calculated with minor computational effort by combining the angle-dependent integral equation theory with the morphometric approach. For example, the calculation for subcomplex III, with ∼27 000 atoms, is finished in only a few seconds on the Xeon workstation.

RESULTS AND DISCUSSION

Water Entropy Gains upon Formation of a Subunit Pair. Table 2 shows the value of $\Delta S_{ij}/k_B$ (see eq 1) for each subunit pair. The values of S_i/k_B and those of S_{ij}/k_B are given in Tables 1S and 2S in the Supporting Information, respectively. ΔS_{ij} represents the water entropy gain upon formation of subunit pair $i-j$. It becomes larger as the tightness of interface packing between subunit pair $i-j$ increases. Therefore, it is a measure of the tightness like the number of stable contacts. It is observed that the order of $\Delta S_{ij}/k_B$ is $\alpha_{TP}-\beta_E < \alpha_E-\beta_E < \alpha_E-\beta_{DP} < \alpha_{DP}-\beta_{TP} < \alpha_{TP}-\beta_{TP} < \alpha_{DP}-\beta_{DP}$ for the $\alpha-\beta$ subunit pairs, $\alpha_{DP}-\gamma < \alpha_{TP}-\gamma < \alpha_E-\gamma$ for the $\alpha-\gamma$ subunit pairs, and $\beta_E-\gamma < \beta_{TP}-\gamma < \beta_{DP}-\gamma$ for the $\beta-\gamma$ subunit pairs.

In Figure 4, we compare the present results with the number of stable contacts estimated by the MD simulation.[32] The correlation coefficient is 0.96, and $\Delta S_{ij}/k_B$ is very well correlated with the number of stable contacts. Thus, the framework of the results of the MD simulation[32] is successfully reproduced using our theoretical method focused on the water entropy effect. In the MD simulation,[32] the Lennard-Jones and Coulomb potentials are fully incorporated, and quite a long computation time is required. On the other hand, since we employ the simple protein model and the morphometric approach, the calculation of the HE for one subunit pair is finished in only a few seconds. Nevertheless, the packing characteristics estimated by the MD simulation can be reproduced beautifully, which is remarkable.

Hydration Entropies of Subcomplexes. Overall conformational changes of the β subunits as well as changes in the interface packing between subunits take place upon the 120° rotation of the γ subunit. For this reason, the three subcomplexes, in each of which one of the β subunits is centered, are more suited to the elucidation of the rotation mechanism. The definitions of the subcomplexes are given in a previous section. Table 3 shows the value of the HE of each subcomplex. It is observed that $|S/k_B|$ is in the order subcomplex III < subcomplex II < subcomplex I. Therefore, the water entropy loss upon the insertion of subcomplex III is the smallest.

The HE value relative to that of subcomplex III is $-626k_B$ for subcomplex I and $-409k_B$ for subcomplex II. These values are quite large. (The former value, for example, corresponds to ∼−1600 kJ/mol at 298 K.) In order to clarify the major physical origin of such large values, we decompose the HE of each subcomplex into intra-subunit and inter-subunit contributions. The intra-subunit contribution is the sum of the HEs of subunits forming each subcomplex, and the inter-subunit contribution is the difference between the HE of each subcomplex and the intra-subunit contribution. The latter represents the contribution from the interface packing between subunits and can be a measure of tight packing between subunits like the number of stable contacts. We discuss the HE, intra-subunit and inter-subunit contributions, and number of stable contacts for each subcomplex given in Table 3. Our principal concern is the value for a subcomplex relative to that for subcomplex III, given in parentheses. As observed in Table 3, the relative values of the intra-subunit contribution for subcomplexes I and II are $-235k_B$ and $-169k_B$, respectively. Each of these values takes only ∼38% (for subcomplex I) or ∼41% (for subcomplex II) of the relative value of the HE; it follows that the relative value of the intersubunit contribution takes ∼62% or ∼59%. This result is indicative that the differences among the subcomplexes in the HE come primarily from the difference in the interface packing between subunits.

The order of the inter-subunit contribution is subcomplex I < subcomplex II < subcomplex III, indicating that the interface packing between subunits is the tightest in subcomplex III. The number of stable contacts in Table 3 is defined as the sum of the numbers of stable contacts between subunits in each subcomplex. This sum and the inter-subunit contribution are in the same order and can well be elucidated in terms of the water entropy effect.

Since the conformations of the complex before and after the 120° rotation of the γ subunit are the same, there is no water entropy change upon the 120° rotation. However, the free energy of the system is reduced by the free-energy decrease resulting from ATP hydrolysis. It is interesting to note that, as observed in Table 3, the rotation leads to water entropy gains of $217k_B$ and $409k_B$ in subcomplex I and subcomplex II, respectively, and a water entropy loss of $626k_B$ in subcomplex III. Strikingly, these values are much larger than the free-energy decrease by ATP hydrolysis, $\sim 12k_BT$. Our result indicates that the apparent interchanges of the water entropy occurring among the three subcomplexes are substantially large, despite the unchanged overall water entropy upon the 120° rotation of the γ subunit.

Hydration Entropies of Subcomplexes *without* the γ Subunit. We calculate the HE of each subcomplex *without* the γ subunit (in this case, subcomplex III, for example, comprises β_{DP}, α_{DP}, and α_E). The results are given in Table 4. It is observed that

dx.doi.org/10.1021/ja109594y | J. Am. Chem. Soc. 2011, 133, 4030–4039

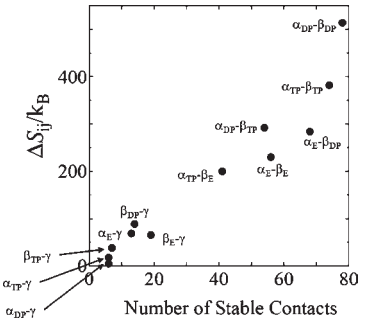

Figure 4. Comparison between the number of stable contacts estimated by the MD simulation with all-atom potentials (see Table 1)[32] and the water entropy gain upon the formation of subunit pair i–j, $\Delta S_{ij}/k_B$ (see Table 2). The correlation coefficient is 0.96, indicating that the two quantities are highly correlated.

Table 4. Hydration Entropy, S/k_B, of each Subcomplex *without* the γ Subunit[a]

subcomplex I (β_E, α_E, and α_{TP})	subcomplex II (β_{TP}, α_{TP}, and α_{DP})	subcomplex III (β_{DP}, α_{DP}, and α_E)
−50 908.5 (−603)	−50 598.2 (−293)	−50 305.7 (0)

[a] The values in parentheses are relative to S/k_B of subcomplex III.

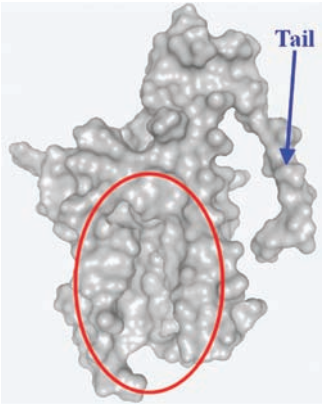

Figure 5. Solvent-surface representation of the native structure of yeast frataxin (PDB ID: 2ga5) drawn by the DS visualizer 2.5. This structure has a large valley, marked by the red ellipse, and a tail, indicated by the blue arrow.

the value of $|S/k_B|$ is in the order subcomplex III < subcomplex II < subcomplex I, which is the same as that in the case *with* the γ subunit observed in Table 3. According to the experimental observation reported by Furuike et al.,[17] the γ subunit retains its rotation in the correct direction as well as its ATP hydrolysis activity even when most of its axle is removed. These results are indicative that the packing in the $\alpha_3\beta_3$ complex *itself* is highly asymmetrical and the order is determined primarily by the asymmetric nature of this complex.

Asymmetric Packing in F_1-ATPase. As explained in Figure 2, it is desired for a protein or a complex of proteins that the backbones and side chains be tightly packed, like a three-dimensional jigsaw puzzle. However, this is not always possible. Even in cases where the overall tight packing is not achievable, there are certainly the portions that can be tightly packed. It is important to pack such portions *preferentially*. For example, the native structure of yeast frataxin[80] has a large valley and a tail, as shown in Figure 5. Nevertheless, $|S|$ of the native structure is almost minimized[49] because the other portions are tightly packed. If an impartial packing was undertaken, the valley and/or the tail could be removed, but the resultant packing would become rather loose, causing a larger value of $|S|$.

The calculation results discussed in the previous subsections strongly indicate that the packing in the $\alpha_3\beta_3\gamma$ complex is highly asymmetrical. The following argument can also be made for the $\alpha_3\beta_3\gamma$ complex: In the situation that two of the β subunits (β_{DP} and β_{TP}) are in closed conformations and the other (β_E) takes an open conformation, the largest decrease in $|S|$ of the $\alpha_3\beta_3$g complex is realized when the tight packing in the γ subunit, β_{DP}, α_{DP}, and α_E, is locally formed (see Figure 3). The packing in the other portions is less important. The overall impartial packing would result in a larger value of $|S|$. The asymmetric packing makes the water entropy almost the largest. In the next subsection, we suggest that the asymmetric packing in the $\alpha_3\beta_3\gamma$ complex plays a crucially important role in the rotation of the γ subunit.

Rotation Mechanism of F_1-ATPase. We first summarize the experimental results that have been reported:

(1) Most of the crystal structures are in the catalytic dwell state.[14−16] Both β_{TP} and β_{DP} are in closed conformations, while β_E adopts an open conformation. We start with Figure 6a, corresponding to the crystal structure shown in Figure 3.

(2) The hydrolysis of ATP in β_{DP}[14] and release of Pi occur[81] with the result that β_{DP} changes its conformation into a half-open one.[16] The β subunit with the changed conformation is denoted β_{DP}^{HO}. The conformational change of β_{DP} leads to the 40° rotation of the γ subunit.[12] The $\alpha_3\beta_3\gamma$ complex now takes the overall conformation shown in Figure 6b. Primes are added to the subunits in Figure 6b because their conformations should be different from those in Figure 6a. Although the crystal structure corresponding to Figure 6b has not been determined yet, it has been shown by single-molecule experiments[16] that β_E', β_{DP}^{HO}, and β_{TP}' are in open, half-open, and closed conformations, respectively.

(3) The conformational changes[16] $\beta_E' \rightarrow \beta_{TP}$ and $\beta_{DP}^{HO} \rightarrow \beta_E$ occur due to the ATP binding[9] and release of ADP,[12] respectively, leading to the 80° rotation of the γ subunit. The $\alpha_3\beta_3\gamma$ complex now takes the overall conformation shown in Figure 6c, which is the same as that of the crystal structure (see Figure 6a). However, the free energy of the system, G_{System}, in Figure 6c is lower than that in Figure 6a because of the free-energy decrease arising from ATP hydrolysis.

Hereafter, we consider the situation where the ATP concentration is much higher than the ADP and Pi concentrations.

Our basic concepts of the rotation mechanism are as follows: (i) the γ subunit rotates so as to suppress the decrease in the water entropy upon the conformational change of a β subunit, and (ii) the γ subunit rotates in such a direction that the tight packing, like that formed by subcomplex III in Figure 6a, can be retained as much as possible. Using concept (i), we can interpret that the 40° rotation of the γ subunit (Figure 6a → Figure 6b), for example, occurs in order to suppress the decrement of the water entropy upon the conformational change of $\beta_{DP} \rightarrow \beta_{DP}^{HO}$. On the basis of concept (ii), we can determine the direction of the rotation of the γ subunit.

We define the orientation of the γ subunit as follows. As shown in Figure 1, the γ subunit has a warped shape with a slightly concave portion and a protruding portion when it is

dx.doi.org/10.1021/ja109594y |*J. Am. Chem. Soc.* 2011, 133, 4030–4039

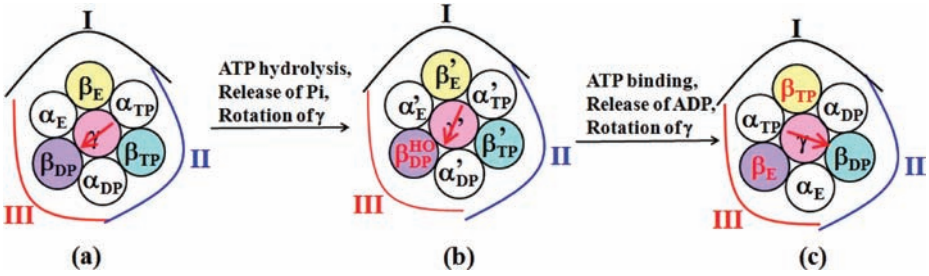

Figure 6. Summary of experimental results using schematic representation of the $\alpha_3\beta_3\gamma$ complex viewed from the F_o side. The crystal structure shown in Figure 1 corresponds to panel (a); panel (b) represents the overall conformation after the first, 40° rotation of the γ subunit, and (c) the overall conformation after the second, 80° rotation of the γ subunit. Primes are added to the subunits in (b) because their conformations should be different from those in (a). The arrow at the center of the γ subunit represents the most tightly packed region.

viewed from the F_o side.[1−5] According to the MD analysis reported by Ito and Ikeguchi,[32] stable contacts are formed between residues Arg8-Ile19 in the γ subunit and residues Asp386-Leu391 in β_{DP}. Residues Arg8-Ile19 are in the slightly concave portion of the γ subunit, indicating that the tight packing is formed between this portion and β_{DP}. This portion is referred to as "portion X" hereafter. The orientation is represented in Figure 6 by the vector linking the centers of the $\alpha_3\beta_3\gamma$ complex and portion X. The vector can be used as a guide to the orientation of the γ subunit. It is important to note that the interface between the γ subunit and β_E interacting with the protruding portion is loosely packed.

The experimental results summarized above can be explained as follows.

(1) Figure 6a: The $\alpha_3\beta_3\gamma$ complex is packed with high asymmetry so that the water entropy in the presence of the $\alpha_3\beta_3\gamma$ complex can be made as high as possible. The tightest packing is formed in subcomplex III. The vector representing the orientation of the γ subunit points toward the most tightly packed region of the $\alpha_3\beta_3\gamma$ complex, subcomplex III.

(2) Figure 6a → Figure 6b: The conformational change of β_{DP} into β_{DP}^{HO}, which follows the hydrolysis of ATP within β_{DP} and release of Pi (both of these, especially the latter, bring a decrease in the system free energy), giving rise to a looser packing in subcomplex III (not only in "β_{DP}, α_{DP}, and α_E" but also between the γ subunit and these subunits). This conformational change would cause a decrease in the water entropy. To suppress the decrease in the water entropy, the structure of the $\alpha_3\beta_3\gamma$ complex is reorganized. In Figure 6a, the water entropy is almost maximized by giving preference to the packing in subcomplex III. However, subcomplex III is no more amenable to such preferential packing, and priority is transferred to the packing in "β_{TP}, α_{TP}, and α_{DP}" or "β_E, α_E, and α_{TP}": a better choice is the former, which is already more tightly packed than the latter. As a consequence, the packing in subcomplex II becomes tighter, while that in subcomplex III becomes looser, which is completed together with the rotation of the γ subunit toward the most tightly packed region, subcomplex II (i.e., by 40° in a counterclockwise direction; the angle 40° comes from the experimental observation). Tight packing like that in subcomplex III in Figure 6a is thus formed with the result that the decrease in the water entropy described above is judiciously suppressed. Since Pi is highly charged, its release leads to a large decrease in the hydration energy. Primarily by this effect, G_{System} in Figure 6b becomes lower than that in Figure 6a.

(3) Figure 6b → Figure 6c: The conformational changes of β_E' and β_{DP}^{HO} ($\beta_E' \rightarrow \beta_{TP}$ and $\beta_{DP}^{HO} \rightarrow \beta_E$) are induced by the ATP binding and ADP release (both of these, especially the former, cause a decrease in the system free energy), respectively. Two of the β subunits are now in closed conformations ,and the other takes an open conformation; the overall conformation, stabilized as shown in Figure 6a, can be recovered. For the recovery, the γ subunit rotates by 80° in a counterclockwise direction: Tight packing like that in subcomplex III can be formed by the rotation to subcomplex II, in which $\beta_{TP}'$is closed. Subcomplex II in Figure 6c forms the tightest packing, which is the same as that in subcomplex III in Figure 6a. The absolute value of the HE of each subcomplex in Figure 6c follows the order subcomplex II < subcomplex I < subcomplex III. The water entropy remains the same upon the overall conformational change, Figure 6a → Figure 6c, but G_{System} is lowered by the free-energy decrease due to ATP hydrolysis.

We remark that G_{System} follows the order Figure 6a > Figure 6b > Figure 6c.

It can be concluded that the highly asymmetrical packing in the $\alpha_3\beta_3\gamma$ complex and the water entropy effect arising from the translational displacement of water molecules induce the rotation of the γ subunit during the chemical processes of ATP binding, ATP hydrolysis, and release of products. The absolute value of the HE of each subcomplex in Figure 6a is in the order subcomplex III < subcomplex II < subcomplex I, which is an increasing function in a counterclockwise direction. That is, the γ subunit rotates in the direction that the absolute value of the HE of the subcomplex increases, and we can know the direction of the rotation by examining the order of $|S|$ for each subcomplex.

According to the rotation mechanism discussed above, the packing in subcomplex III becomes looser upon the 40° or 80° rotation. This would lead to a water entropy loss. The water entropy loss, which is much larger than the free-energy gain by ATP hydrolysis (it reaches $626k_B$ upon the 120° rotation), must be compensated so that the free energy of the system can decrease upon the 40° or 80° rotation. In this case, the water entropy loss is compensated by the water entropy gain brought by the tighter packing in the other subcomplexes accompanying the rotation of the γ subunit. Thus, we can conclude that the rotation is induced to compensate for the water entropy loss.

Furuike et al.[17] showed that the rotation of the γ subunit is retained even when most of the axle of the γ subunit is removed. This experimental result suggests that rotation of the γ subunit can be induced primarily by the asymmetric packing of the $\alpha_3\beta_3$ complex. It is observed from Tables 3 and 4 that the order of $|S/k_B|$ of the subcomplex without the γ subunit is the same as that of the subcomplex with γ subunit: β_{DP}-α_{DP}-α_E > β_{TP}-α_{TP}-α_{DP} > β_E-α_E-α_{TP}. In our opinion, the rotation mechanisms with

dx.doi.org/10.1021/ja109594y |*J. Am. Chem. Soc.* 2011, 133, 4030–4039

and without the γ subunit share essentially the same physical substance.

It is experimentally known that the $\alpha_3\beta_3$ complex without the γ subunit and nucleotides takes an symmetric conformation.[82] According to the crystal structure obtained by Kabaleeswaran et al., the packing of the $\alpha_3\beta_3\gamma$ complex becomes asymmetric even in the absence of nucleotides,[6] indicating that the asymmetric packing of the $\alpha_3\beta_3\gamma$ complex arises from the twisted and asymmetric structure of the γ subunit.[1] The experimental result reported by Furuike et al.[17] suggests that the packing of the $\alpha_3\beta_3$ complex is asymmetrical due to nonuniform binding of nucleotides to the three β subunits. We can conclude from these experimental results that the asymmetric packing of the $\alpha_3\beta_3\gamma$ complex arises from the asymmetric nature of the γ subunit and/or nonuniform binding of nucleotides to the three β subunits. Perturbations such as ATP binding, ATP hydrolysis, and release of the products induce the transition from one asymmetric packing to another, accompanying the rotation of the γ subunit. When the γ subunit is forced to be rotated by the F_o part, the γ subunit induces the transition between different asymmetric conformations of the $\alpha_3\beta_3$ complex, leading to the ATP synthesis. Thus, F_1-ATPase works owing to the asymmetric packing arising mainly from the water entropy effect.

Comments on Direct Interaction between Subunits. A tight packing leads to a decrease in the intramolecular energy by van der Waals and electrostatic attractive interactions among the protein atoms. We note, however, that the tight packing leads to a loss of attractive interactions with water molecules, leading to an increase in the protein−water interaction energy, the so-called dehydration penalty.[36,38−40] The intramolecular-energy decrease is largely compensated by the dehydration penalty. This has been verified by a theoretical analysis using the 3D-RISM theory combined with all-atom potentials comprising Lennard-Jones and Coulomb terms and the SPC/E water model.[83] Furthermore, the dehydration penalty can become even larger when salts are added to water.[84] There is experimental evidence that, for apoPC folding,[52] the dehydration penalty is dominant and the enthalpy change is positive. Thus, the tight packing is not likely to be ascribed to an energy decrease in the system. Since the framework of the results of the MD simulation with all-atom potentials comprising Lennard-Jones and Coulomb terms[32] is reproducible by the water entropy effect alone, it is probable that the energetic components are not important in forming the asymmetric packing in F_1-ATPase and inducing the rotation of the γ subunit.

Two kinds of direct interactions between the γ and β subunits have been proposed as important factors for the rotation: Ma et al.[24] have suggested that the electrostatic interaction between Arg and Lys residues on the protruding portion of the γ subunit and negatively charged residues of the β subunit, known as the DELSEED motif, plays essential roles in the rotation. As explained above, however, such an energetic component can hardly be a principal factor inducing the rotation. Furthermore, Hara et al. have shown that the rotation is not influenced by the mutation of residues in the DELSEED motif to Ala,[85] indicating that the electrostatic interaction between the γ and β subunits plays no important roles for the rotation. The other direct interaction proposed as an important factor for the rotation is the steric repulsion between the γ subunit and the set of β subunits.[29,30] Studies using a coarse-grained model[29,30] have shown that even when only the repulsive interaction between them is taken into consideration, the conformational change of the set of β subunits induces the rotation of the γ subunit. It should be noted, however, that an artificial potential is required to avoid flying-out of the γ subunit from the central cavity formed by the $\alpha_3\beta_3$ complex (see the Supporting Information of ref 30). Thus, it is doubtful that the $\alpha_3\beta_3\gamma$ complex is stabilized only by the steric repulsion between the γ subunit and the set of β subunits. Furthermore, according to the experimental result reported by Fruike et al.,[17] the γ subunit retains its rotation in the correct direction as well as its ATP hydrolysis activity even when most of its axle is removed. This gives further evidence of the unimportance of the two kinds of direct interactions discussed above.

CONCLUSION

We have performed extensive analyses on the $\alpha_3\beta_3\gamma$ complex of F_1-ATPase. First, the water entropy gains upon the formation of the $\alpha-\beta$, $\alpha-\gamma$, and $\beta-\gamma$ subunit pairs are calculated. The gain is given as the difference between the hydration entropy (HE) of a subunit pair and the sum of the HEs of separate subunits forming the subunit pair. The water entropy gain is considered as a measure of tightness of the packing at each subunit interface. The results are highly correlated with the numbers of stable contacts at the subunit interfaces, estimated by a molecular dynamics (MD) simulation with all-atom potentials comprising Lennard-Jones and Coulomb terms,[32] which demonstrates the validity of our theoretical method based on the water entropy effect. Second, three different subcomplexes comprising the γ subunit, one of the β subunits, and the two α subunits adjacent to them are defined, and the HEs of these subcomplexes are calculated. The HEs thus obtained are remarkably different from one another. A smaller absolute value of the HE means a smaller loss of the water entropy upon the insertion of the subcomplex. The loss originates from a decrease in the total volume available to the coexisting water molecules and resultant reduction in the number of accessible configurations of the water. A smaller absolute value of the HE is ascribed to a tighter packing in the subcomplex. We find that the packing in the $\alpha_3\beta_3\gamma$ complex is highly asymmetrical. In all the calculations, we employ a hybrid of the angle-dependent integral equation theory[59−61] combined with the multipolar water model[62,63] and the morphometric approach.[64,65]

On the basis of the calculation results, we have proposed the mechanism of rotation of the γ subunit. In our picture, the asymmetric packing of the $\alpha_3\beta_3\gamma$ complex and the water entropy effect arising from the translational displacement of water molecules induce the rotation during the chemical processes of the ATP binding, ATP hydrolysis, and release of products. From the viewpoint of structural chemistry, the $\alpha_3\beta_3$ complex possesses three-fold symmetry, and there should be three different overall conformations retaining the highly asymmetrical packing. Here we discuss the mechanism of the 40° rotation of the γ subunit from the crystal structure (i.e., Figure 6a → Figure 6b) as an example. In the crystal structure, the γ subunit, β_{DP}, and two adjacent α subunits (subcomplex III in Figure 3a) form a tight packing. However, the conformational change of β_{DP} results in a looser packing in subcomplex III. The water entropy would decrease as a result of this looser packing. In order to suppress the water entropy decrease, a tighter packing in one of the other regions must be formed with the help of rotation of the γ subunit in the direction of the more tightly packed region (according to the experimental result, by 40° in a counterclockwise direction

when F_1-ATPase is viewed from the F_o side). Our scheme would be strengthened if we could use the crystal structure corresponding to Figure 6b; however, this structure has not been determined yet. In future work, the conformation of the $\alpha_3\beta_3\gamma$ complex corresponding to Figure 6b could be generated using an MD simulation.

This is the first time that the HEs of F_1-ATPase, its subunits, and its subunit pairs are calculated using a molecular model for water. Calculation of the HE of F_1-ATPase using the MD simulation with all-atom potentials is almost impossible at present due to the huge computation time required. On the other hand, angle-dependent integral theory is hard to apply to a protein because of its mathematical complexity. Since we combine angle-dependent integral equation theory with the morphometric approach in our theoretical method, the calculation is finished in only a few seconds. Furthermore, our method has the advantage that an infinite number of water molecules and the protein−water−water triplet and higher-order correlations are explicitly incorporated via the angle-dependent integral equation theory. Its reliability has been demonstrated for a variety of important protein-related problems.[35−41,44−51] It is remarkable that, as shown in Figure 4, we have succeeded in reproducing the framework of the results of MD simulation.[32] Our method can be applied to very large proteins and protein complexes such as F_1-ATPase and actomyosin (i.e., myosin and F-actin).

The water entropy effect has been shown to be the key factor in elucidating folding/unfolding mechanisms of proteins.[33−51] We have recently reported new progress in uncovering the mechanism of the unidirectional movement of a linear-motor protein (e.g., myosin) along a filament (e.g., F-actin).[86] The unidirectional movement of the linear-motor protein is also controlled by the water entropy effect. It has also been shown that the insertion of a large solute into a vessel constructed of biopolymers (e.g., the import of a polypeptide into the chaperonin GroEL and that of an antibiotic molecule or a toxic protein into a cell-membrane protein) is driven by the water entropy effect.[87] Thus, the water entropy effect is imperative for a variety of biological processes sustaining life.

■ ASSOCIATED CONTENT

Supporting Information. Details of the model of water; angle-dependent integral equation theory; procedure for determining the four coefficients in the morphometric approach; Tables S1 and S2, showing the values of the hydration entropies of subunits and subunit pairs, respectively; and complete ref 69. This material is available free of charge via the Internet at http://pubs.acs.org.

■ AUTHOR INFORMATION

Corresponding Author
kinoshit@iae.kyoto-u.ac.jp

■ ACKNOWLEDGMENT

The computer program for the morphometric approach was developed with Roland Roth and Yuichi Harano. This work was supported by Grants-in-Aid for Scientific Research on Innovative Areas (Nos. 20118004 and 21118519), on Priority Areas (No. 18074004), and on (B) (Nos. 22300100 and 22300102) from the Ministry of Education, Culture, Sports, Science and Technology of Japan and by the Grand Challenges in Next-Generation Integrated Simulation of Nanoscience and Living Matter, a part of the Development and Use of the Next-Generation Supercomputer Project of MEXT.

■ REFERENCES

(1) Abrahams, J. P.; Leslie, A. G.; Lutter, R.; Walker, J. E. *Nature* **1994**, *370*, 621.
(2) Gibbons, C.; Montgomery, M. G.; Leslie, A. G. W.; Walker, J. E. *Nat. Struct. Biol.* **2000**, *7*, 1055.
(3) Menz, R. I.; Walker, J. E.; Leslie, A. G. *Cell* **2001**, *106*, 331.
(4) Kabaleeswaran, V.; Puri, N.; Walker, J. E.; Leslie, A. G. W.; Mueller, D. M. *EMBO J.* **2006**, *25*, 5433.
(5) Bowler, M. W.; Montgomery, M. G.; Leslie, A. G. W.; Walker, J. E. *J. Biol. Chem.* **2007**, *282*, 14238.
(6) Kabaleeswaran, V.; Shen, H.; Symersky, J.; Walker, J. E.; Leslie, A. G. W.; Mueller, D. M. *J. Biol. Chem.* **2009**, *284*, 10546.
(7) Noji, H.; Yasuda, R.; Yoshida, M.; Kinosita, K., Jr. *Nature* **1997**, *386*, 299.
(8) Yasuda, R.; Noji, H.; Kinosita, K., Jr.; Yoshida, M. *Cell* **1998**, *93*, 1117.
(9) Yasuda, R.; Noji, H.; Yoshida, M.; Kinosita, K., Jr.; Itoh, H. *Nature* **2001**, *410*, 898.
(10) Shimabukuro, K.; Yasuda, R.; Muneyuki, E.; Hara, K. Y.; Kinosita, K., Jr.; Yoshida, M. *Proc. Natl. Acad. Sci. U.S.A.* **2003**, *100*, 14731.
(11) Nishizaka, T.; Oiwa, K.; Noji, H.; Kimura, S.; Muneyuki, E.; Yoshida, M.; Kinosita, K., Jr. *Nat. Struct. Mol. Biol.* **2004**, *11*, 142.
(12) Adachi, K.; Oiwa, K.; Nishizaka, T.; Furuike, S.; Noji, H.; Itoh, H.; Yoshida, M.; Kinosita, K., Jr. *Cell.* **2007**, *130*, 309.
(13) Ariga, T.; Muneyuki, E.; Yoshida, M. *Nat. Struct. Mol. Biol.* **2007**, *14*, 841.
(14) Okuno, D.; Fujisawa, R.; Iino, R.; Hirono-Hara, Y.; Imamura, H.; Noji, H. *Proc. Natl. Acad. Sci. U.S.A.* **2008**, *105*, 20722.
(15) Sieladd, H.; Rennekamp, H.; Engelbrecht, S.; Junge, W. *Biophys. J.* **2008**, *95*, 4979.
(16) Masaike, T.; Koyama-Horibe, F.; Oiwa, K.; Yoshida, M.; Nishizaka, T. *Nat. Struct. Mol. Biol.* **2008**, *15*, 1326.
(17) Furuike, S.; Hossain, M. D.; Maki, Y.; Adachi, K.; Suzuki, T.; Kohori, A.; Itoh, H.; Yoshida, M.; Kinosita, K., Jr. *Science* **2008**, *319*, 955.
(18) Shimo-Kon, R.; Muneyuki, E.; Sakai, H.; Adachi, K.; Yoshida, M.; Kinosita, K., Jr. *Biophys. J.* **2010**, *98*, 1227.
(19) Toyabe, S.; Okamoto, T.; Watanabe-Nakayama, T.; Taketani, H.; Kudo, S.; Muneyuki, E. *Phys. Rev. Lett.* **2010**, *104*, 198103.
(20) Hayashi, K.; Ueno, H.; Iino, R.; Noji, H. *Phys. Rev. Lett.* **2010**, *104*, 218103.
(21) Watanabe, R.; Iino, R.; Noji, H. *Nat. Chem. Biol.* **2010**, *6*, 814.
(22) Itoh, H.; Takahashi, A.; Adachi, K.; Noji, H.; Yasuda, R.; Yoshida, M.; Kinosita, K., Jr. *Nature* **2004**, *427*, 465.
(23) Böckmann, R. A.; Grubmuller, H. *Nat. Struct. Mol Biol.* **2002**, *9*, 198.
(24) Ma, J.; Flynn, T. C.; Cui, Q.; Leslie, A. G. W.; Walker, J. E.; Karplus, M. *Structure* **2002**, *10*, 921.
(25) Böckmann, R. A.; Grubmuller, H. *Biophys. J.* **2003**, *85*, 1482.
(26) Yang, W.; Gao, Y. Q.; Cui, Q.; Ma, J.; Karplus, M. *Proc. Natl. Acad. Sci. U.S.A.* **2003**, *100*, 874.
(27) Dittrich, M.; Hayashi, S.; Schulten, K. *Biophys. J.* **2003**, *85*, 2253.
(28) Dittrich, M.; Hayashi, S.; Schulten, K. *Biophys. J.* **2004**, *87*, 2954.
(29) Koga, N.; Takada, S. *Proc. Natl. Acad. Sci. U.S.A.* **2006**, *103*, 5367.
(30) Pu, J.; Karplus, M. *Proc. Natl. Acad. Sci. U.S.A.* **2008**, *105*, 1192.
(31) Ito, Y.; Ikeguchi, M. *Chem. Phys. Lett.* **2010**, *490*, 80.
(32) Ito, Y.; Ikeguchi, M. *J. Comput. Chem.* **2010**, *31*, 2175.
(33) Harano, Y.; Kinoshita, M. *Chem. Phys. Lett.* **2004**, *399*, 342.
(34) Harano, Y.; Kinoshita, M. *Biophys. J.* **2005**, *89*, 2701.
(35) Harano, Y.; Roth, R.; Kinoshita, M. *Chem. Phys. Lett.* **2006**, *432*, 275.

(36) Harano, Y.; Roth, R.; Sugita, Y.; Ikeguchi, M.; Kinoshita, M. *Chem. Phys. Lett.* **2007**, *437*, 112.
(37) Yoshidome, T.; Kinoshita, M.; Hirota, S.; Baden, N.; Terazima, M. *J. Chem. Phys.* **2008**, *128*, 225104.
(38) Kinoshita, M. *Int. J. Mol. Sci.* **2009**, *10*, 1064.
(39) Kinoshita, M. *Front. Biosci.* **2009**, *14*, 3419.
(40) Yoshidome, T.; Oda, K.; Harano, Y.; Roth, R.; Sugita, Y.; Ikeguchi, M.; Kinoshita, M. *Proteins: Struct., Funct. Genet.* **2009**, *77*, 950.
(41) Yasuda, S.; Yoshidome, T.; Oshima, H.; Kodama, R.; Harano, Y.; Kinoshita, M. *J. Chem. Phys.* **2010**, *132*, 065105.
(42) Harano, Y.; Kinoshita, M. *J. Phys.: Condens. Matter.* **2006**, *18*, L107.
(43) Harano, Y.; Kinoshita, M. *J. Chem. Phys.* **2006**, *125*, 024910.
(44) Harano, Y.; Yoshidome, T.; Kinoshita, M. *J. Chem. Phys.* **2008**, *129*, 145103.
(45) Yoshidome, T.; Harano, Y.; Kinoshita, M. *Phys. Rev. E* **2009**, *79*, 011912.
(46) Yoshidome, T.; Kinoshita, M. *Chem. Phys. Lett.* **2009**, *477*, 211.
(47) Yoshidome, T. *Entropy* **2010**, *12*, 1632.
(48) Yoshidome, T.; Kinoshita, M. *Phys. Rev. E* **2009**, *79*, 030905(R).
(49) Oshima, H.; Yoshidome, T.; Amano, K.; Kinoshita, M. *J. Chem. Phys.* **2009**, *131*, 205102.
(50) Amano, K.; Yoshidome, T.; Harano, Y.; Oda, K.; Kinoshita, M. *Chem. Phys. Lett.* **2009**, *474*, 190.
(51) Oda, K.; Kodama, R.; Yoshidome, T.; Yamanaka, M.; Sambongi, Y.; Kinoshita, M. *J. Chem. Phys.* **2011**, *134*, 025101.
(52) Baden, N.; Hirota, S.; Takabe, T.; Funasaki, N.; Terazima, M. *J. Chem. Phys.* **2007**, *127*, 175103.
(53) Ohtaka, H.; Schon, A.; Freire, E. *Biochemistry* **2003**, *42*, 13659.
(54) Kardos, J.; Yamamoto, K.; Hasegawa, K.; Naiki, H.; Goto, Y. *J. Biol. Chem.* **2004**, *279*, 55308.
(55) Bonafe, C. F.; Vital, C. M.; Telles, R. C.; Goncalves, M. C.; Matsuura, M. S.; Pessine, F. B.; Freitas, D. R.; Vega, J. *Biochemistry* **1998**, *37*, 11097.
(56) Kasai, M.; Asakura, S.; Oosawa, F. *Biochim. Biophys. Acta* **1962**, *57*, 13.
(57) Swezey, R. R.; Somero, G. N. *Biochemistry* **1982**, *21*, 4496.
(58) Kauzmann, W. *Adv. Protein Chem.* **1959**, *14*, 1.
(59) Hansen, J.-P.; McDonald, I. R. *Theory of Simple Liquids*; Academic Press: London, 1986.
(60) Kinoshita, M. *J. Chem. Phys.* **2008**, *128*, 024507.
(61) Kinoshita, M.; Yoshidome, T. *J. Chem. Phys.* **2009**, *130*, 144705.
(62) Kusalik, P. G.; Patey, G. N. *J. Chem. Phys.* **1988**, *88*, 7715.
(63) Kusalik, P. G.; Patey, G. N. *Mol. Phys.* **1988**, *65*, 1105.
(64) König, P. M.; Roth, R.; Mecke, K. R. *Phys. Rev. Lett.* **2004**, *93*, 160601.
(65) Roth, R.; Harano, Y.; Kinoshita, M. *Phys. Rev. Lett.* **2006**, *97*, 078101.
(66) Oroguchi, T.; Hashimoto, H.; Shimizu, T.; Sato, M.; Ikeguchi, M. *Biophys. J.* **2009**, *96*, 2808.
(67) Sali, A.; Blundell, T. L. *J. Mol. Biol.* **1993**, *234*, 779.
(68) Imai, T.; Harano, Y.; Kinoshita, M.; Kovalenko, A.; Hirata, F. *J. Chem. Phys.* **2006**, *125*, 024911.
(69) MacKerell, Jr.; et al. *J. Phys. Chem. B* **1998**, *102*, 3586.
(70) Lee, B.; Richards, F. M. *J. Mol. Biol.* **1971**, *55*, 379.
(71) Connolly, M. L. *J. Appl. Crystallogr.* **1983**, *16*, 548.
(72) Connolly, M. L. *J. Am. Chem. Soc.* **1985**, *107*, 1118.
(73) Ikeguchi, M.; Doi, J. *J. Chem. Phys.* **1995**, *103*, 5011.
(74) Kinoshita, M. *J. Chem. Phys.* **2002**, *116*, 3493.
(75) Kötting, C.; Kallenbach, A.; Suveyzdis, Y.; Wittinghofer, A.; Gerwert, K. *Proc. Natl. Acad. Sci. U.S.A.* **2008**, *105*, 6260.
(76) Asakura, S.; Oosawa, F. *J. Chem. Phys.* **1954**, *22*, 1255.
(77) Asakura, S.; Oosawa, F. *J. Polym. Sci.* **1958**, *33*, 183.
(78) Lazaridis, T.; Paulaitis, M. E. *J. Phys. Chem.* **1992**, *96*, 3847.
(79) Lazaridis, T.; Paulaitis, M. E. *J. Phys. Chem.* **1994**, *98*, 635.
(80) Adinolfi, S.; Nair, M.; Politou, A.; Bayer, E.; Martin, S.; Temussi, P.; A. Pastore, A. *Biochemistry* **2004**, *43*, 6511.
(81) There are two schemes for the release of Pi:[12] Pi produced from ATP hydrolysis is released immediately,[18] or the release is suspended for the next 120° rotation.[21] The release of Pi occurs from the β_{DP} subunit in the former picture, while it occurs from the β_{E} subunit in the latter picture.
(82) Shirakihara, Y.; Leslie, A. G.; Abrahams, J. P.; Walker, J. E.; Ueda, T.; Sekimoto, Y.; Kambara, M.; Saika, K.; Kagawa, Y.; Yoshida, M. *Structures* **1997**, *5*, 825.
(83) Imai, T.; Harano, Y.; Kinoshita, M.; Kovalenko, A.; Hirata, F. *J. Chem. Phys.* **2007**, *126*, 225102.
(84) Kinoshita, M.; Harano, Y. *Bull. Chem. Soc. Jpn.* **2005**, *78*, 1431.
(85) Hara, K. Y.; Noji, H.; Bald, D.; Yasuda, R.; Kinosita, K., Jr.; Yoshida, M. *J. Biol. Chem.* **2000**, *275*, 14260.
(86) Amano, K.; Yoshidome, T.; Iwaki, M.; Suzuki, M.; Kinoshita, M. *J. Chem. Phys.* **2010**, *133*, 045103.
(87) Amano, K.; Kinoshita, M. *Chem. Phys. Lett.* **2010**, *488*, 1.